Magnetic Pendulum: Dynamical Systems and Chaos with the Fast Lyapunov Indicator

PEREZ Jérome[1] and ELKALACHE Georges[1]

[1]Applied Mathematics Unit, ENSTA Paris, Palaiseau, 91120, France

June 30, 2024

Abstract

Studying physics for the last three decades showed that the representation and analysis of simple and natural phenomenons most often require advanced mathematics and abstract theories. Newton for instance found himself compelled to develop calculus to formalize his analysis. A similar pattern can be tracked all the way to quantum physics' linear algebra. In the same sense, the study of the game-like magnetic pendulum presented in this paper introduces variational dynamics' Fast Lyapunov Indicator (FLI) and Poincaré maps in an attempt to classify its behavior in the chaotic realm. Although the system is deterministic, meaning its motion is described using deterministic equations, it seems to be very sensitive to initial conditions which we tried to quantify both theoretically and experimentally in this study. Few articles have been published on the subject of this particular system, however, none of them uses the Fast Lyapunov Indicators as chaos indicator. This recently introduced tool will be used as the main tool for this study where will be exploring its advantages, potential use cases and the accuracy of the results.

1 Introduction

The device is simple : a magnetic bob at the end of a string hanging freely above N base-plane magnets. Placed in position $r_0 = (x_0, y_0)$ in the base plane, once liberated, the pendulum follows a path specific to the initial position. How specific? This is what the paper tries to determine. The equations that govern its motion are given by classical mechanics. Assuming that the length of the pendulum is much greater than the distance between the hanging mass and the base, the motion can be considered plane. Moreover, this allows us to only consider small angles and thus a gravitational force $\vec{F}_{\text{grav}} \propto -w^2\vec{r}$ where we will choose $w = 1$ for the rest of the study. The effect of the magnets on the pendulum will be modeled using the dipole approximation considering that the magnets' size is insignificant compared to other magnitudes involved. Thus,

$$\vec{F}_{\text{mag}} \propto \sum_{n=1}^{N} \frac{\epsilon_n(\vec{r}_n - \vec{r})}{(|\vec{r}_n - \vec{r}|^2 + h^2)^{\frac{5}{2}}}$$

where $\vec{r}_n$ represents the position vector of the magnet n and $\vec{r}$ the position of bob at an instant t. ϵ_n represents the orientation of the magnetic momentum of each magnet; $\epsilon_n = +1$ for a repulsive magnet, $\epsilon_n = -1$ for an attractive one. h is introduced as a regulatory parameter to avoid divergence when the bob is directly above a magnet.To finish up with the forces, the choice of taking friction into consideration or lack thereof will change the type of the dynamical system and thus its behavior. The two approaches will be elaborated on in details later in the study, using $\vec{F}_{\text{friction}} \propto -\beta\frac{d\vec{r}}{dt}$ where β is the friction coefficient. Newton's second law provides us with the following motion equation

$$\frac{d^2\vec{r}}{dt^2} = -\vec{r} - \frac{\beta}{m}\frac{d\vec{r}}{dt} + \frac{1}{m}\sum_{n=1}^{N} \frac{\epsilon_n(\vec{r}_n - \vec{r})}{(|\vec{r}_n - \vec{r}|^2 + h^2)^{\frac{5}{2}}} \tag{1.1}$$

2 Chaos Indicators : Lyapunov Analysis

2.1 Definitions

One of the most important properties a system must verify to qualify as chaotic is extreme sensitivity to initial conditions. This is to say that minimal change in initial conditions results in very different outcomes. The butterfly effect " does the flap of a butterfly's wings in Brazil set off a tornado in Texas " by Edward Lorentz [1] is a well known concept illustrating this phenomenon, presenting climate as a clear representation of a chaotic dynamical system. Regarding the magnetic pendulum, classical mechanics' deterministic laws predict that the equilibrium point of the pendulum is going to be above one of the magnets. Since the movement is considered plane in this study, we can say that the equilibrium position is going to be one of the magnets'. The different outcome we spoke about is thus, in our case, a different trajectory and eventually "landing on" a different magnet.

As illustrated below, we launch the experiment for 4 values of y differing by 0.001 where $x = -0.5$, T =100 and $\alpha = 0.05$. The magnet of color green is the one representing the equilibrium point or the final state of the pendulum. The impact of this small variation in y_0 is clear and is what essentially drove researchers to dive deeper into the study of this system and use advanced mathematical tools and concepts in order to collect more information regarding its behavior.

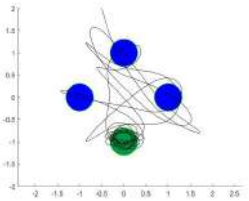

Figure 1: $y_0 = 1.998$

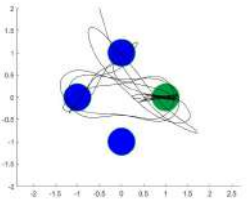

Figure 2: $y_0 = 1.997$

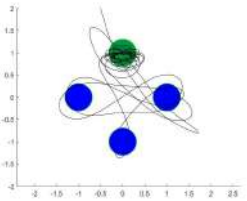

Figure 3: $y_0 = 1.996$

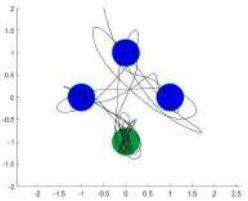

Figure 4: $y_0 = 1.995$

The main challenge faced when studying dynamical systems is that apart from trivial cases, we don't know how to find an explicit analytical solution. As a result, we study chaos in dynamical systems by means of cartography : in a space of initial conditions, we attempt to locate the regions giving chaotic, regular or resonant solutions. To do that, numerous mathematical tools called chaos indicators are available. The main tool used in this study is going to be the Fast Lyapunov Indicator (FLI) introduced by Froeschlé and al. [2] as an alternative to Lyapunov Characteristic Exponents (LCE). LCE are chaos indicators widely used when working with variational dynamics and orbits' chaoticity; for the given dynamical system, the deviation vector w verifies the linearized equation

$$\begin{cases} \dot{x} = f(x) \\ \dot{w} = \frac{\partial f}{\partial x} w \end{cases}$$

The Lyapunov Exponent is thus defined

$$\mathrm{LCE}(x_0, w_0) := \lim_{t \to \infty} \frac{1}{t} \ln \left(\frac{\|w(t)\|}{\|w(0)\|} \right)$$

For chaotic Hamiltonian systems, the largest LCE is always strictly positive. For instance, the largest LCE of a linear system is almost always its biggest eigenvalue. The main issue with LCEs is the long computation time especially in the case of weak chaos [3]

The Fast Lyapunov Indicator is thus introduced [4] given that (as its name indicates) it is significantly faster to compute yet it stills allows us to quantify choaticity levels

$$FLI_{u(0)} := \sup_{0 \leq t \leq T} \ln \frac{\|w_j(t)\|}{\|w(0)\|}, \quad j \in 1, ..., 2n \tag{2.1}$$

2.2 Differential System

For the same dynamical system, considering a non-dissipative approach where $\beta = 0$ and m = 1, we introduce $\mathbf{u} = [x, y, p_x, p_y]^\top$. The system is now Hamiltonian with two degrees of liberty, and $\mathbf{u}$ verifies the Hamiltonian equation

$$\dot{\mathbf{u}} = f(\mathbf{u}) = J \operatorname{grad}_{\mathbf{u}} H(\mathbf{u}) \tag{2.2}$$

where $H(\mathbf{u}) = \frac{1}{2}\|\mathbf{u}\|^2 - \frac{1}{3}\sum_{n=1}^{N} \frac{\epsilon_n}{(\|\mathbf{u}-\mathbf{u}_n\|^2+h^2)^{\frac{3}{2}}}$, $\mathbf{u}_n = [x_n, y_n, p_x, p_y]^\top$ and $J = \begin{bmatrix} 0_2 & I_2 \\ -I_2 & 0_2 \end{bmatrix}$, I_2 and 0_2 being the identity and the null matrices respectively.

A perturbation vector w tangent to the dynamic $\mathbf{w} = [\delta x, \delta y, \delta p_x, \delta p_y]^\top$ verifying

$$\dot{\mathbf{w}} = Df\,(\mathbf{u})\mathbf{w} \tag{2.3}$$

where $Df(\mathbf{u})$ is the differential of the Hamiltonian flow

$$Df\,(\mathbf{u}) = \begin{bmatrix} 0 & 0 & 1 & 0 \\ 0 & 0 & 0 & 1 \\ A(x,y) & B(x,y) & 0 & 0 \\ B(x,y) & C(x,y) & 0 & 0 \end{bmatrix} \qquad \begin{aligned} A(x,y) &= \frac{\partial(f(\mathbf{u})\cdot\mathbf{e}_3)}{\partial x} \\ B(x,y) &= \frac{\partial(f(\mathbf{u})\cdot\mathbf{e}_3)}{\partial y} \\ C(x,y) &= \frac{\partial(f(\mathbf{u})\cdot\mathbf{e}_4)}{\partial y} \end{aligned}$$

Given that $Df(\mathbf{u})$ is a function of t through $x(t)$ and $y(t)$, in order to integrate (4) we have to integrate (3) first. We thus attempt to integrate both simultaneously introducing $\mathbf{z} = [\mathbf{u}, \mathbf{w}]^\top \in \mathbb{R}^8$ verifying the following equation

$$\dot{\mathbf{z}} = F(\mathbf{z}) \tag{2.4}$$

Once $\mathbf{z}(t)$ is computed for a given initial vector $\mathbf{z}_0 = [\mathbf{u}_0, \mathbf{w}_0]^\top$ where we will choose $\mathbf{w}_0 = \frac{1}{2}[1,1,1,1]$ and $|\mathbf{w}_0| = 1$, we can finally compute the FLI. It is clear that the FLI is a function of the initial condition. For a fixed time span T, $\mathbf{w}_0$, p_x and p_y, computing the FLI for every point in the plane returns a number that quantifies how chaotic the point's vicinity is. Doing that helps us identify patterns and regions of regularity on the map [5].

3 Simulation and Results

In order to plot the map we first need to specify the time span T of the experiment, the number and positions of the magnets and a discretization factor K fixing the number of initial conditions to be considered. The system has to solve K*K*T differential equations for each map.

3.1 Results

All the obtained FLI maps confirm the chaotic nature of the system with positive FLI values ranging from 0 to 600. The map is divided into several zones, indicating the sensitivity of each to initial conditions. Clearly visible in the adjacent figure is a sort of boundary layer that envelops the domain of the magnets. In this vicinity, the pendulum will have enough energy to reach the influence zones of the other magnets, thus having a greater number of "path choices" than a pendulum released directly above a magnet, which will attract it towards itself, leaving it little chance to gain kinetic energy and move away.

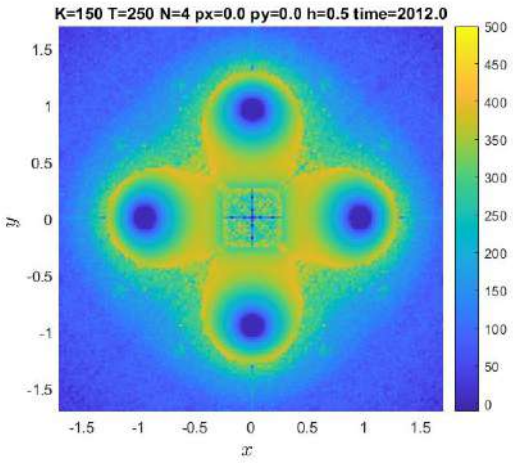

3.2 Parameters Influence

In the following section we explore the impact of each parameter on the end result and visualize the FLI map. In all of the tests, unless otherwise stated, $\epsilon_n = +1$, the integrator's fixed time step is 0.5, 4 magnets are present, h = 0.5, $\mathbf{w}_0$ is as previously fixed and $p_x = p_y = 0$

A- Variation of time span T

It is important to know the suitable value of T for conducting the simulations. Although the main reason for using the FLI is the short calculation time compared to other indicators, imposing a short simulation duration may result in outcomes that do not reflect the real behavior. To find the ideal T that balances time and information, we conducted the experiment for 4 consecutive values, t being the execution time of the code:

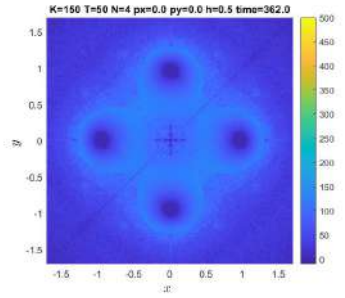

Figure 5: K = 150, T = 50

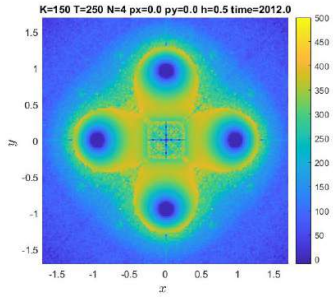

Figure 6: K = 150, T = 150

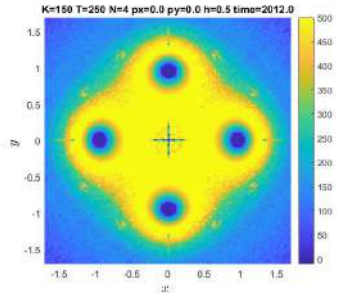

Figure 7: K = 150, T = 250

It is clear that the chaoticity becomes more evident and pronounced as the duration of the experiment increases. For T = 150, we get a clear view of the contrasted regions with a practical execution time. You will notice that in the rest of the study, we always choose T around 150. In the following paragraph, T = 100 is chosen to reduce the effect of chaos over time to better visualize the variation of chaos caused by the variation of h.

B- Variation of added parameter h

The regulatory parameter h introduced to the denominator of the magnetic effect's expression has a proportionate effect on the surface occupied by each magnet, and thus has an inversely proportionate influence on the degree of chaos, as clearly visualized below; for h=0.1 (figure 8), which is closest to the real case of h=0, the system is much more chaotic than for h=0.4 (figure 11), noting that the square of h is taken into account in the expression.

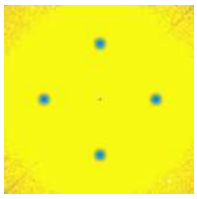

Figure 8: 0.1

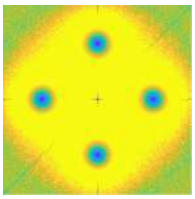

Figure 9: 0.2

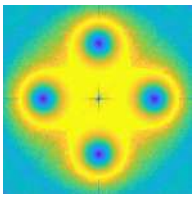

Figure 10: 0.3

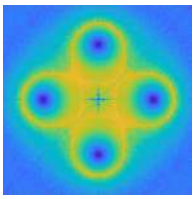

Figure 11: 0.4

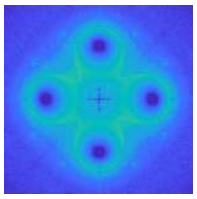

Figure 12: 0.5

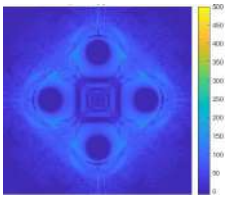

Figure 13: 0.6

C- Variation of spatial configuration and magnet number

It is quite intuitive that chaos is proportional to the number of magnets, given that the presence of a magnet offers a new path for the pendulum to choose. This is especially true when the magnets are close to each other without overlapping. For fewer than 3 magnets, the system is not really interesting to study. The choice of 4 magnets arranged in a cross on the axes is due to a preference for generality and symmetry. Here we test different configurations to verify the consistency of the model and the lack of bias in the adopted configuration.

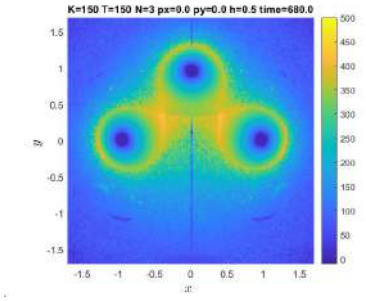

Figure 14: K = 150, T = 50

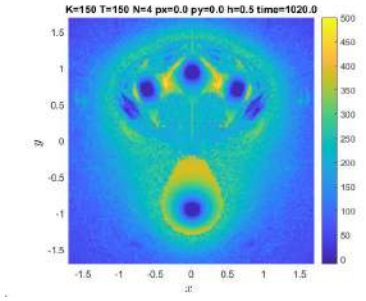

Figure 15: K = 150, T = 150

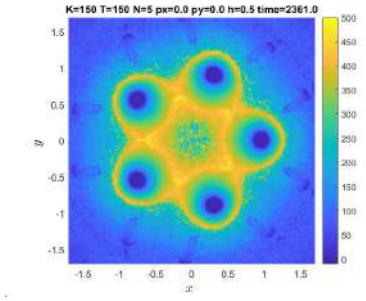

Figure 16: K = 150, T = 250

4 Poincaré Sections

The use of Poincaré sections is widespread in the study of nonlinear continuous dynamical systems, particularly in the context of chaos. A Poincaré section is a hyperplane in the state space of a system. The points on this plane are intersections of different orbits that the system can trace with the considered hyperplane. Exploring this plane, which provides a temporally discrete dynamical representation, allows us to draw conclusions about the nature of the dynamics and identify regions of regular, periodic, and chaotic behavior [5].

A plane densely filled with points indicates unstable orbits that rarely pass through the same point, unlike a plane where structured and empty regions show some periodicity. Finite-time indicators such as FLI can be used to represent the phase space of a system, from which Poincaré sections can be deduced, enabling the study of motion distribution between predictability and chaos [3].

We will now compute Poincaré sections using the FLI. This involves fixing a hyperplane (e.g., x=0) and the system's energy.

4.1 Hénon-Heiles

Initially, we apply this to the Hénon-Heiles system, whose section form is already known [6], in order to test the code:

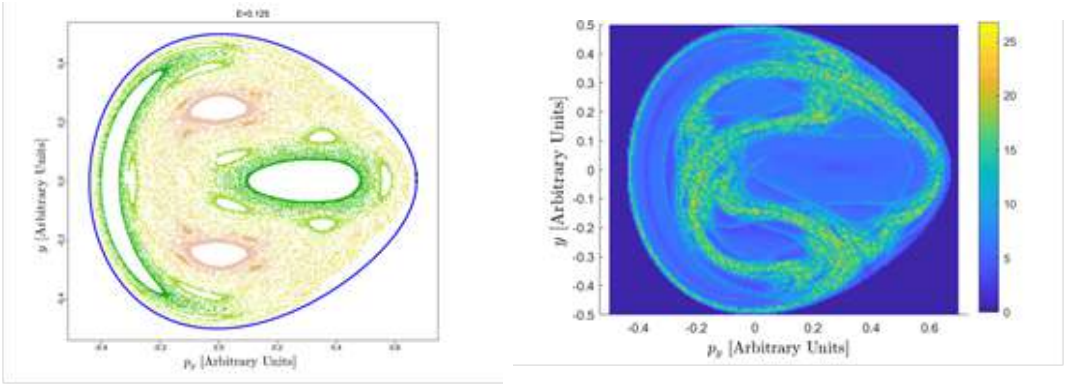

Figure 17: E = 0.125, 100 initial conditions, intersection with the plane $x = 0,\ p_x = 0$

The difference typically arises because the Poincaré section (left) depends on the number of initial conditions and orbits considered, where for each condition we have a section map and all the maps are eventually combined to obtain the overall figure. With the FLI method, one intersection gives us the complete representation, since the computation of FLI maps already involves all possible initial conditions (those that are not fixed) and trajectories.

4.2 Magnetic Pendulum

For the magnetic pendulum, Poincaré sections were obtained for specific energy values, and results were compared with those obtained using FLI. Increasing the energy revealed structured patterns, which makes sense as higher pendulum velocities reduce the impact of magnets, thereby decreasing chaotic regions filled with points. This can be observed when comparing sections for E = 3 and E = 5.

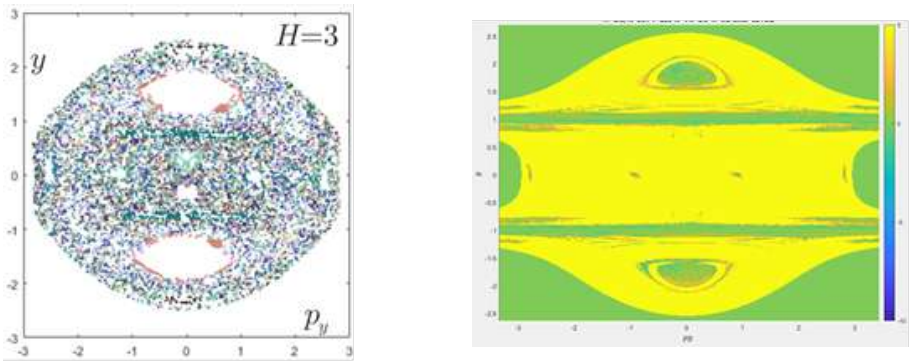

Figure 18: E = 3, 10 initial conditions, E=0, intersection with the plane $x = 0,\ p_x = 0$

On the left, we observe the section plotted for E=3, and on the right, the figure for the same parameters plotted using FLI. The structures indicating regularity zones are common to both figures, although the stability of these regions may vary slightly, especially with the presence of numerical singularities caused by the computational divergence. Fast Lyapunov Indicators thus provide the complete section with reduced computation time and complexity. Further exploration involves changing the value of the energy E and the number of initial conditions considered.

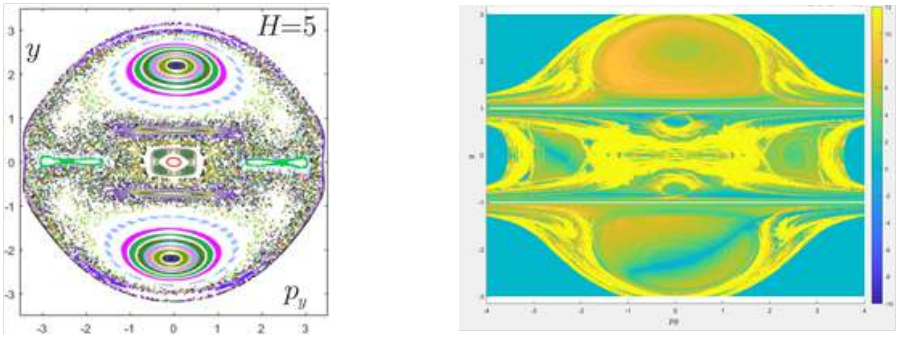

Figure 19: E = 5, 25 initial conditions, intersection with the plane $x = 0,\ p_x = 0$

Similarities between these maps are easily detected. We can spot similar geometrical structures forming in the same regions. In this Poincaré section, the evidence is empirical and does not prove nor generalise the direct relation between traditional sections and those done with FLI, but results are very promising and we believe that, more research done in this area, the computational efficiency of FLI will have significantly bigger influence on the domain of chaos and dynamical systems.

5 Non-dissipative approach $\beta \neq 0$

The work presented before this paragraph is based on the motion equation (1.1) which does not take dissipation into consideration ($\beta = 0$), allowing us to conduct the study on a Hamiltonian system. Now that chaos was detected in the ideal model, we need to verify if this result can be extended to the real system, and detect the parameters that come into play. An attempt will thus be done using WADA Basins. The motion equation, having $\alpha = \frac{\beta}{m}$, is :

$$\frac{d^2\vec{r}}{dt^2} = -\vec{r} - \alpha\frac{d\vec{r}}{dt} + \sum_{n=1}^{N} \frac{\epsilon_n(\vec{r}_n - \vec{r})}{(|\vec{r}_n - \vec{r}|^2 + h^2)^{\frac{5}{2}}} \tag{5.1}$$

5.1 WADA Basin

An interesting property often found in dissipative nonlinear dynamical systems appears on our system if we establish the following figure: having 3 magnets, we associate each magnet with a color (red, blue, and green). In a space of initial conditions, each starting point is colored by the color of the magnet on which the dynamics stabilize. We observe the following result :

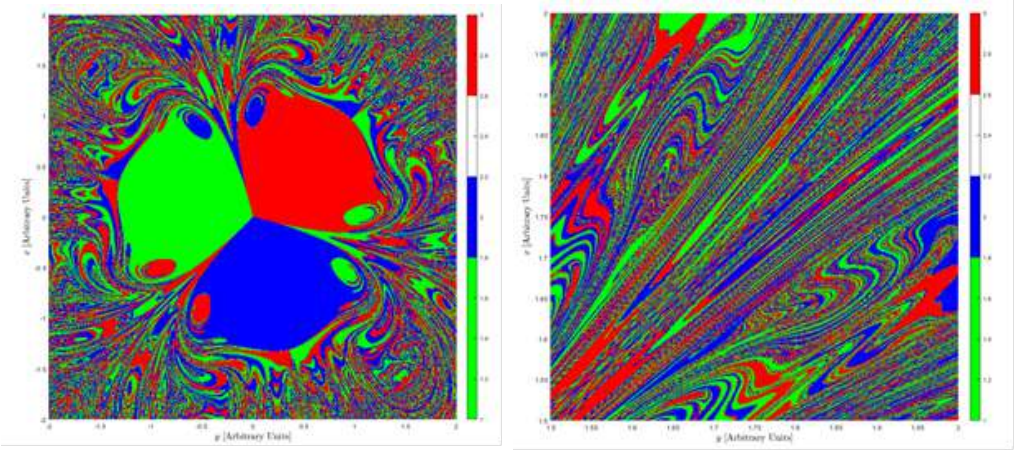

Figure 20: Attraction basin for 3 magnets, $\alpha = 0.1$, $d = 1$, $h = 0.5$, $p_0 = (0, 0)$ and K = 500 making it a (500 x 500) map

The topology of these maps are similar to the structure of WADA basins. WADA basins are regions in the phase space of a dynamical system where three or more basins of attraction are intertwined in such a way that every point on the boundary of one basin is also on the boundary of all the others [7]. This property is known as the WADA property. In other words, no matter how much you zoom in on the boundary of one basin, you will always find points from at least three different basins. In simpler words, to move from the basin of color 1 to the basin of color 2, one must always pass through the basin of color 3 [8]. If we can mathematically prove that the considered system verifies the WADA property, we can confirm that the system remains chaotic in the dissipative case [9]. This demonstration remains the subject of further research and exploration.

5.2 Influence of damping parameter α

Usually friction kills chaos. In the previous map we saw that chaos remains. The fractal aspect is less remarkable as we increment α, the damping parameter, as seen in the figures below (figure 22 and figure 23). This highlights the importance of choosing a realistic value for α in order to have the most accurate map.

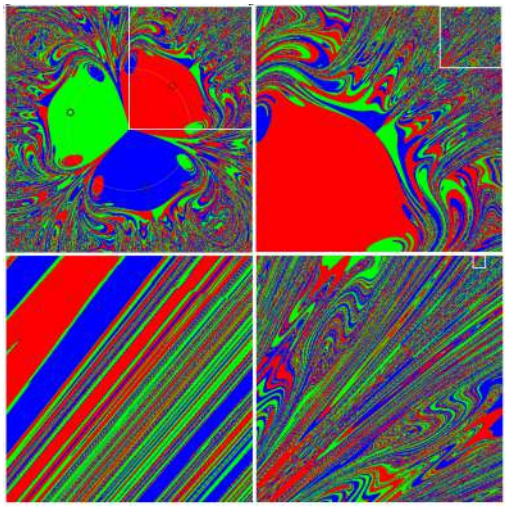

Figure 21: $\alpha = 0.1$

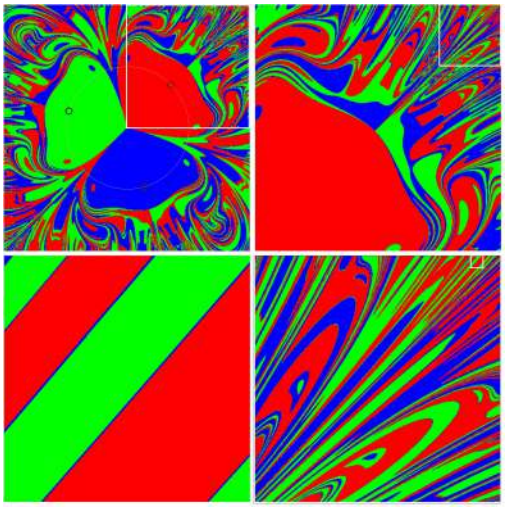

Figure 22: $\alpha = 0.15$

5.3 Experimental study

With the importance of the damping parameter α being previously highlighted, an experimental device representing the magnetic pendulum was made available and was used to attempt on finding the actual value of α. We were able to launch many tests and track the evolution of the trajectory and the energy of the system. Given that the experimental exponential decay of the energy is the negative of the theoretical friction parameter, we were able to compute a value for α :

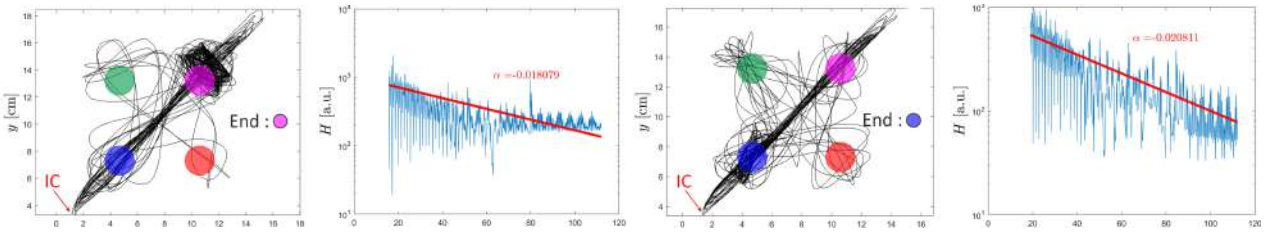

Figure 23: Samples of the experimental results

From a large set of various data we get $\alpha = 0.0189 \pm 0.003$. This value is even smaller than the one used for figure 22 - $\alpha = 0.1$ where the map already exhibit fractal structures indicating chaos. This is to say that the experimental results align with the theoretical ones given by the computation of Fast Lyapunov Indicators in the space of initial conditions.

6 Conclusion

The magnetic pendulum, a rather simple and amusing toy, remains a four-dimensional non-linear problem in phase space after simplifications. The phenomenon of sensitivity to initial conditions is often encountered in nature and carries important information about the system, as we have just seen. The exploration of the FLI chaos indicator gave us an idea of the effectiveness of this tool in this domain and its relation to other chaos quantification methods, particularly Poincaré sections. In ideal conditions, the pendulum exhibits strongly chaotic behavior, as explored in our simulations. The extension of this result to damping scenarios seems very probable, and still needs robust investigation and ideally mathematical proofs concerning the WADA property and the role of fractal geometry in certain representations. Although this particular system does not contribute much technologically or industrially, its simplicity leave room for great understanding and appropriation of the FLI, which would certainly be useful for applications on dynamic systems, most notably the study of stability of satellite orbits, but can also make use to understand the dynamics of non linear mathematical models for finance and neuroscience.

References

[1] E. Lorenz. Predictability; does the flap of a butterfly's wings in brazil set off a tornado in texas? 1972.

[2] L. G. Froeschlé. The fast lyapunov indicator: A simple tool to detect weak chaos. *Elsevier Science*, Ltd 45, 1997.

[3] J. Daquin. Computation of phase portraits with the fast lyapunov indicator.

[4] C. Froeschlé and E. Lega. On the structure of symplectic mappings. the fast lyapunov indicator: A very sensitive tool. In *New Developments in the Dynamics of Planetary Systems*, pages 167–195. Springer, 2001.

[5] Perez J. *Théorie des Champs Classiques*. Les presses de l'Ensta, 2017.

[6] M. Taramgini. Some notes on the henon-heiles hamiltonian system.

[7] Kennedy J. and Yorke J.A. Basins of wada. *Physica D*, 51:213–225, 1991.

[8] H.E. Nusse and J.A. Yorke. Basins of attraction. *Science*, 271:1376–1380, 1996.

[9] J. M. C. C. FIMA and H. A. J. Middleton-Spencer. Chaos in the magnetic pendulum. *Mathematics Today*, 2020.